

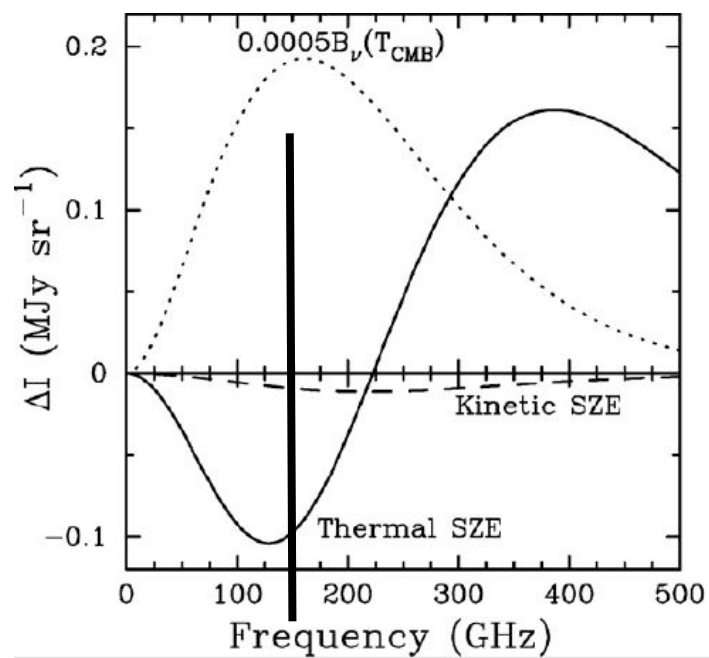
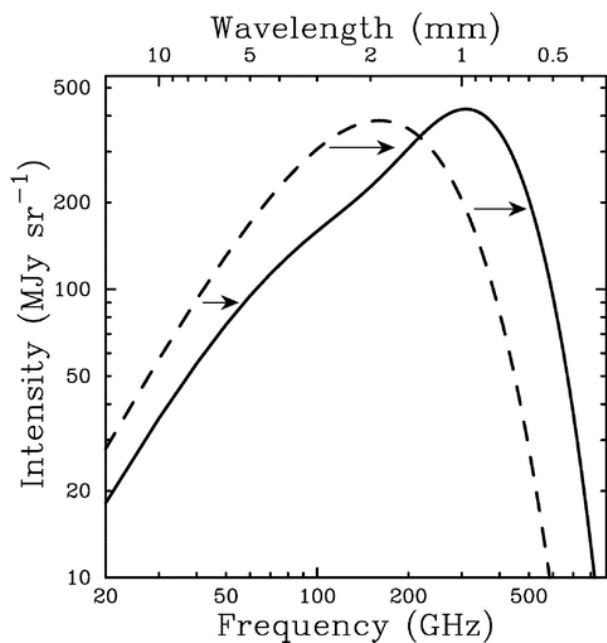
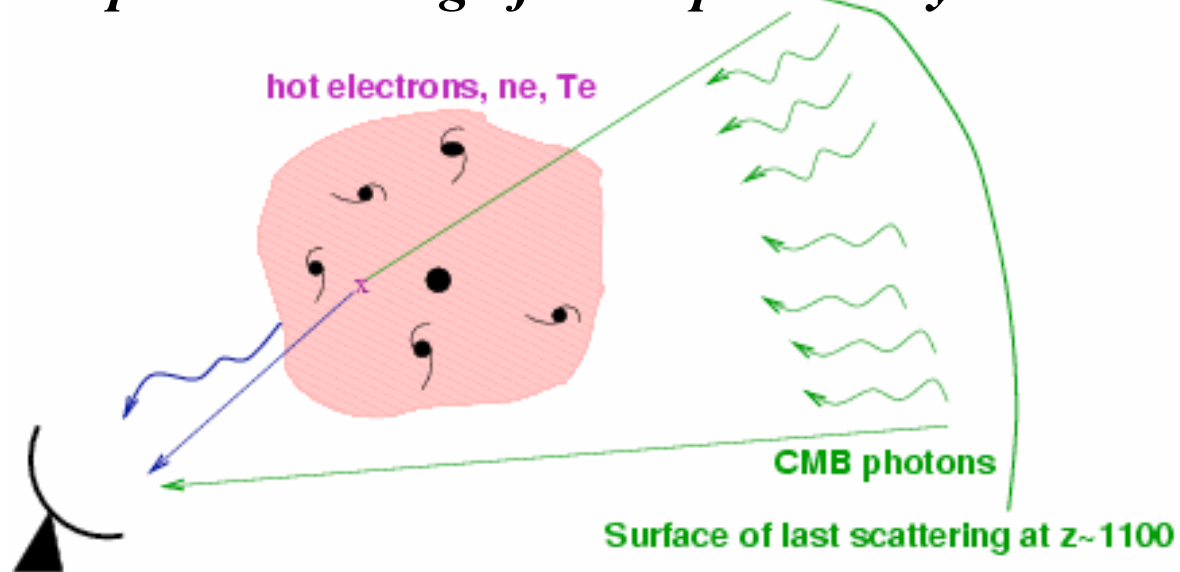
APEX-SZ observations of galaxy clusters

Cathy Horellou, Onsala Space Observatory / Chalmers

- Mapping the SZ decrement at 2 mm (150 GHz)
- Angular resolution of 1'; FOV = 24'
- Observations between 2005 and 2010
- 48 clusters + 2 deep fields.



Inverse Compton scattering of CMB photons by hot electrons



Charateristic distortions of the CMB spectrum:

1. Thermal SZ effect

Decrement in the radio/mm,
increment in the submm

$$\Delta T_{\text{SZ,th}}/T_{\text{CMB}}(\nu) \propto \int_{\text{cluster}} n_e T_e dl = \text{gas pressure}$$

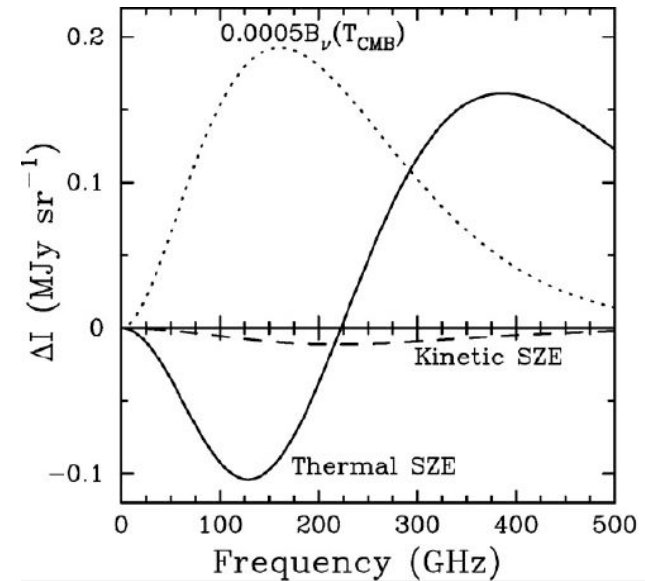
2. Kinetic SZ effect: 10 times weaker

$$\Delta T_{\text{SZ,kin}}/T_{\text{CMB}}(\nu) \propto -v_{\text{pec}}/c$$

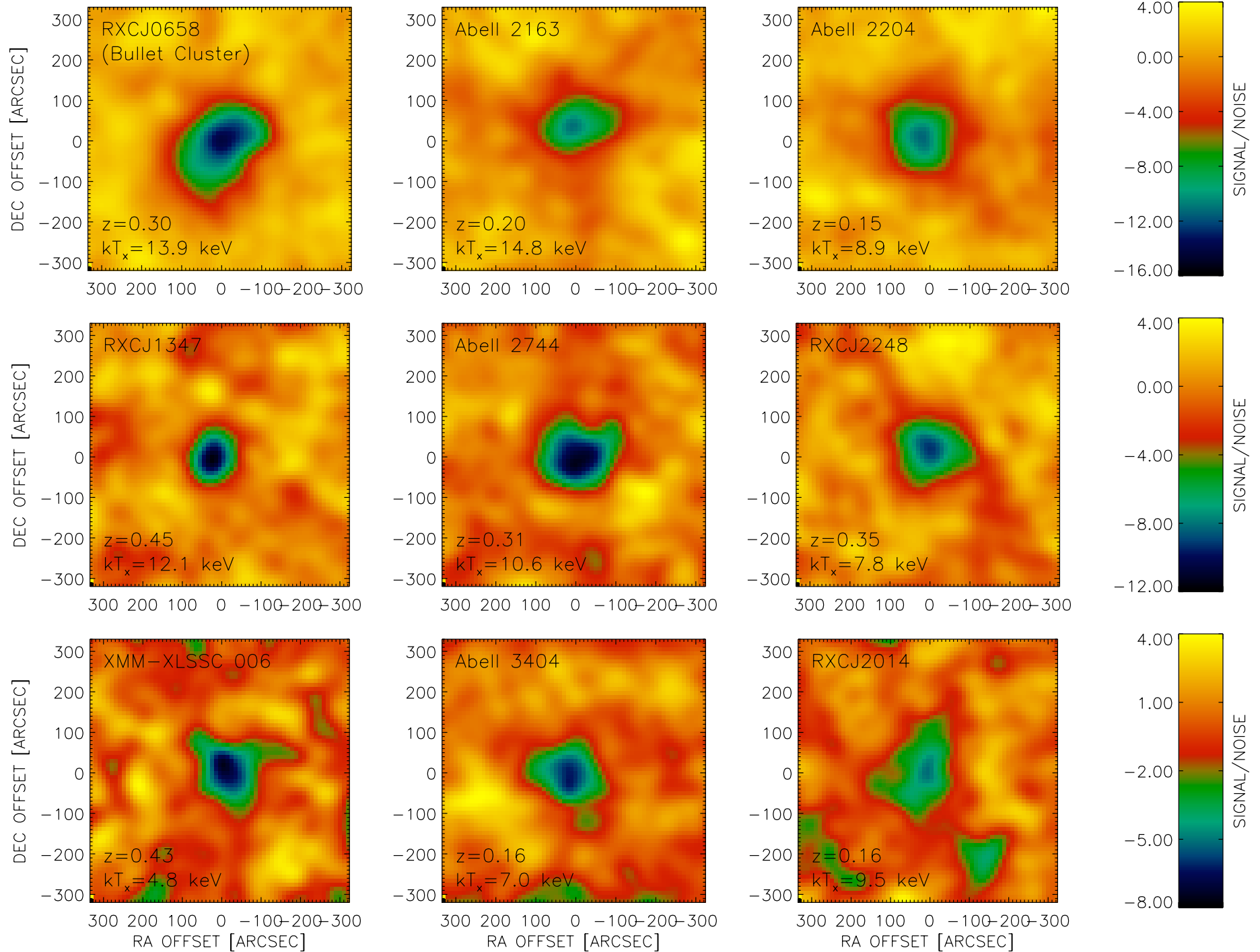
Depends on the **mass** of the intracluster gas.

Current observations are sensitive to clusters with masses $M > \text{a few } 10^{14} M_{\text{sun}}$.

Important: independent of redshift!



Example of APEX-SZ 150 GHz maps (M. Nord, PhD thesis)



The Atacama Pathfinder EXperiment, APEX

- A 12 m telescope at 5100 m elevation near the ALMA site
- Partners: ESO (24%), Germany (45%), Sweden (21%), Chile (10%)
- Versatile instrument:
 - Nasmyth A cabin:
 - 4 spectral-line receivers, 211-1390 GHz (facility instruments)
 - FLASH (spectral-line receiver, 280-510 GHz; MPIfR PI instrument)
 - Nasmyth B cabin:
 - Champ+ (spectral-line receiver, 602-950 GHz, German PI instrument)
 - Cassegrain cabin: 3 bolometer cameras
 - SABOCA 350 micron (facility instrument)
 - LABOCA 870 micron (facility instrument)
 - APEX-SZ (ASZCA) at 2 mm (German PI instrument, built at U of California)
 - 2-4 weeks per year since 2007 (920 hours on source, German+Swedish time)

The APEX-SZ collaboration

UC Berkeley / LBNL

Hsiao-Mei Cho
John Clarke
Daniel Ferrusca
Bill Holzapfel
Zigmund Kermish
Adrian Lee
Martin Lueker
Jared Mehl
Tom Plagge
Christian Reichardt
Paul Richards
Dan Schwan
Helmuth Spieler
Ben Westbrook
Martin White
Oliver Zahn

NASA Goddard

Brad Johnson

Boulder Colorado

Amy Bender
Nils Halverson

Mc Gill University, Canada

Matt Dobbs
James Kennedy
Trevor Lanting

Bonn University

Frank Bertoldi
Matthias Klein
Florian Pacaud
Martin Sommer
Reinhold Schaaf

Max-Planck Institute for Radio Astronomy, Bonn

Kaustuv Basu
Rolf Guesten
Ernst Kreysa
Karl Menten
Dirk Muders
Felipe Navarrete

Max-Planck Institute for Extraterrestrial Physics, Munich

Hans Boehringer
Gayong Chon
Rene Fassbender

Onsala/Chalmers

Cathy Horellou
Daniel Johansson

ESO Santiago

Ruediger Kneissl

Outline

- **The APEX-SZ camera, observing strategy and data analysis**
 - Instrument paper (Schwan et al. 2011, Rev. of Sci. Instr., in press)
- **The dataset**
- **Published results**
 - The Bullet Cluster (Halverson et al. 2009, ApJ)
 - Abell 2163, dual-frequency 150 + 345 GHz SZ observations (Nord et al. 2009, A&A)
 - Abell 2204, joint X-ray-SZ analysis, de-projection, non-parametric modeling (Basu et al. 2010, A&A)
 - Power spectrum of the central 0.8 square degrees of the XMM-LSS field (Reichardt et al. 2009, ApJ);
- **Work in progress**
 - SZ-mass scaling relations (Bender et al., Klein et al.)
 - The merging cluster Abell 2744 (Horellou et al.)
 - Contaminating point sources
 - *[Stacking analysis to probe the outskirts of relaxed clusters (Basu et al.)]*
 - *Substructures (Kennedy et al.)*
 - ...
- **Future work**
 - *[ALMA+ACA, CCAT,] LOFAR*

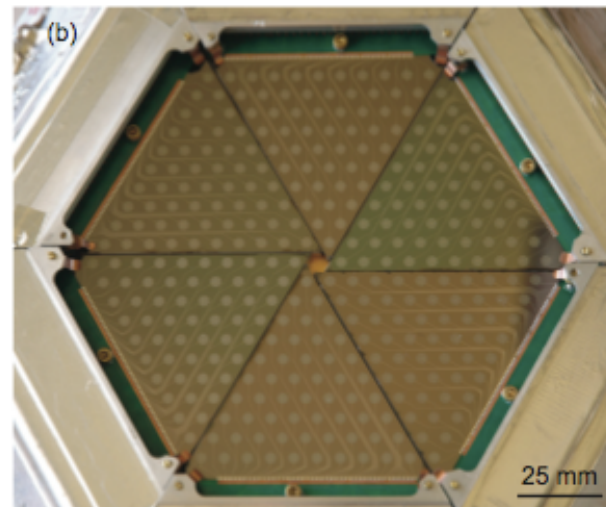
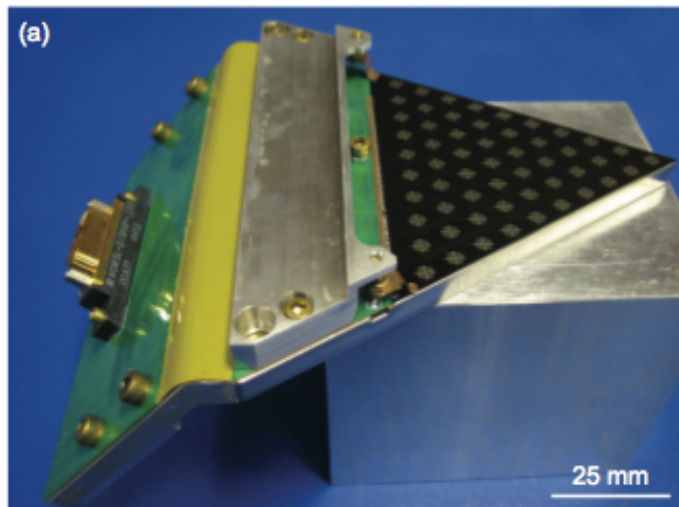
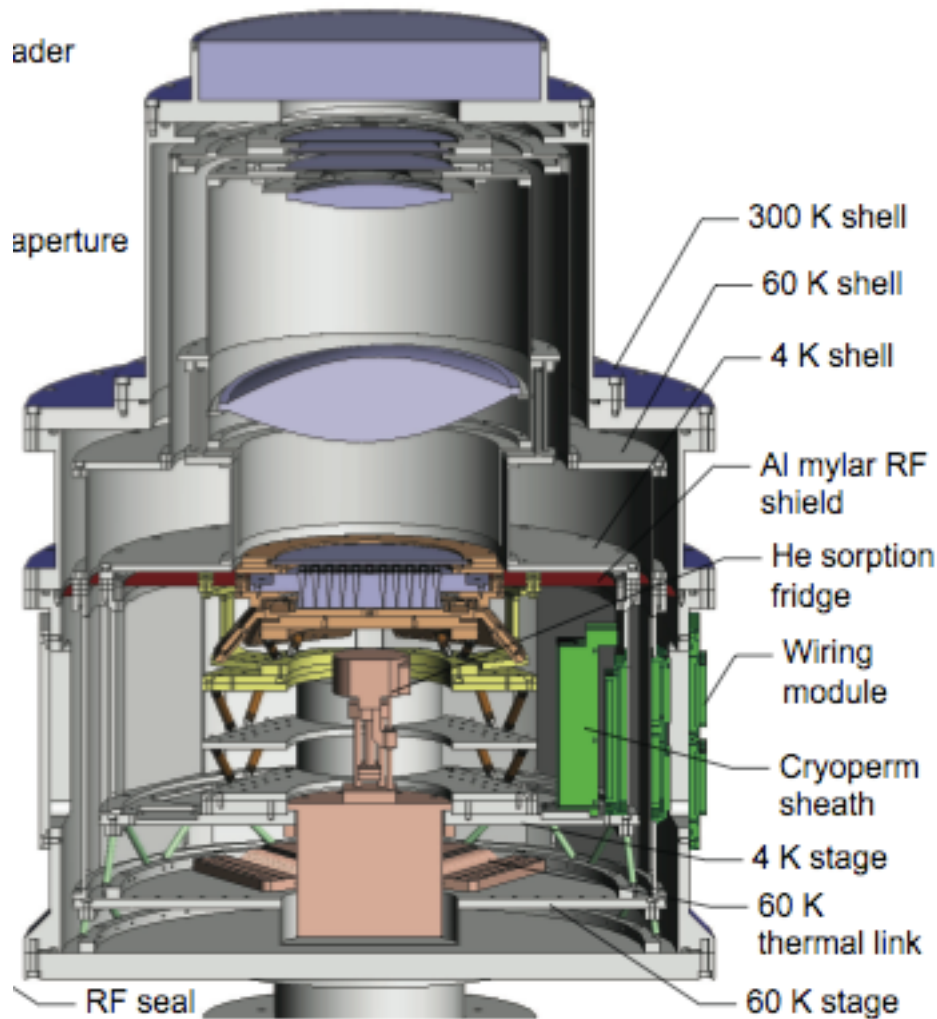
Schwan et al. 2011, in press

New technologies pioneered in APEX-SZ:

- Transition edge sensors (TES)
- Frequency-domain multiplexed readout
- Use of a pulse-tube cooler

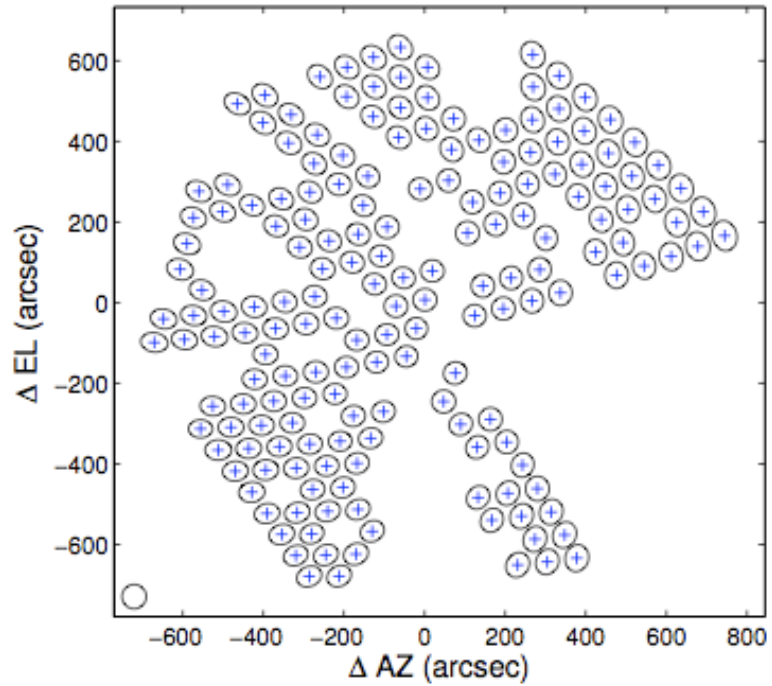
330 bolometers in total,
280 bolometers wired

Drawing of the cryostat

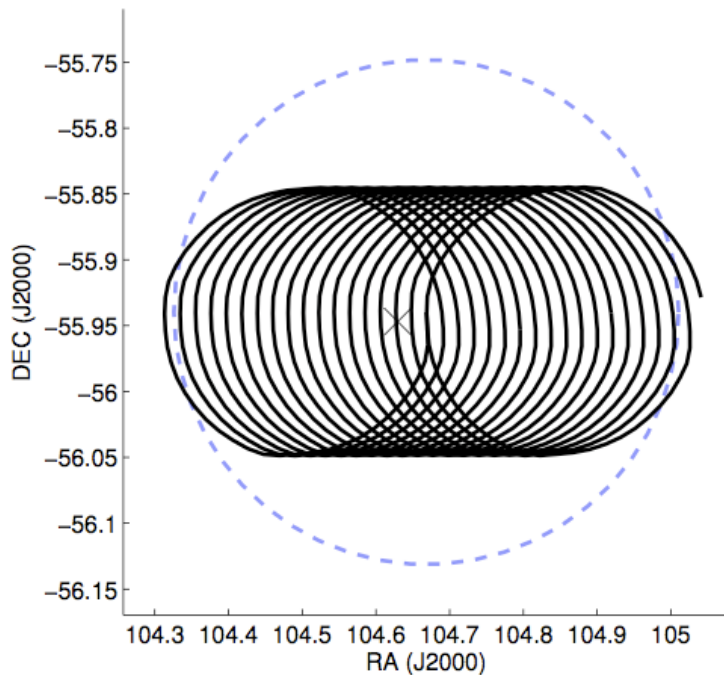


6 wedges of
55 bolometers each

From time streams to a 2D image of the SZ brightness



Fit of elliptical Gaussian beams to
177 optically live bolometers



Circular drift scan pattern with a
diameter of 6 to 12 arcmin
Duration of a circle: 4-10 s

The dataset

Total time spent on science targets by APEX-SZ

The list is sorted by right ascension.

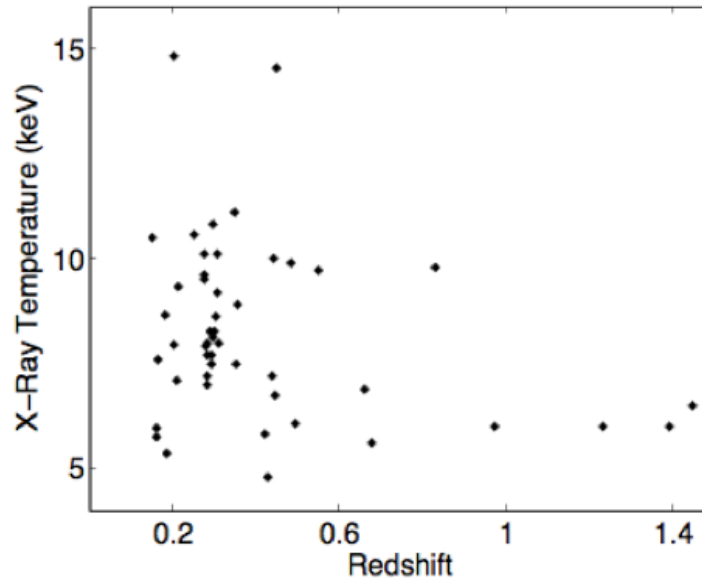
OBJECT	R.A.	Dec	mar07	apr07	aug07	dec07	may08	nov08	apr09	dec09	nov10	TOTAL
A2744	00:14:18.8	-30:23:00	-	-	-	-	7.8	-	-	-	14.5	22.2
RXCJ0019.0-2026	00:19:07.8	-20:27:21	-	-	-	-	-	-	-	-	8.5	8.5
CL0024+17	00:26:35.6	+17:09:44	-	-	-	-	-	-	1.4	-	-	1.4
A2813	00:43:24.4	-20:37:17	-	-	-	-	-	0.5	-	-	8.1	8.7
A209	01:31:52.6	-13:36:37	-	-	-	-	-	-	-	-	8.9	8.9
XMM-LSS-2	02:21:05.7	-03:37:48	-	-	-	31.2	-	-	-	-	-	31.2
XLSSC-006	02:21:45.1	-03:46:19	-	-	43.3	-	-	-	-	-	-	43.3
RXCJ0232.2-4420	02:32:18.7	-44:20:41	-	-	-	-	-	-	-	8.7	-	8.7
RXCJ0245.4-5302	02:45:27.7	-53:02:10	-	-	-	-	-	0.2	12.9	-	-	13.1
A383	02:48:03.6	-03:32:09	-	-	-	-	-	8.3	-	-	7.0	15.3
RXCJ0437.1+0043	04:37:09.8	+00:43:37	-	-	-	-	-	-	-	-	9.9	9.9
MS0451.6-0305	04:54:11.4	-03:00:52	-	-	-	-	-	-	8.3	-	-	8.3
A520	04:54:19.0	+02:56:49	-	-	-	-	11.2	-	-	-	10.6	21.8
RXCJ0516.6-5430	05:16:38.0	-54:30:51	-	-	-	-	-	-	16.1	9.9	-	26.0
RXCJ0528.9-3927	05:28:52.5	-39:28:16	-	-	-	-	-	-	14.4	6.3	-	20.7
RXCJ0532.9-3701	05:32:55.9	-37:01:35	-	-	0.9	-	-	-	13.7	7.6	-	22.2
A3404	06:45:29.3	-54:13:08	-	-	4.7	-	4.0	-	-	-	5.3	14.1
Bullet	06:58:31.1	-55:56:49	1.3	2.5	7.6	-	-	-	-	-	-	11.5
RXCJ0956.4-1004	09:56:26.4	-10:04:12	-	-	-	-	-	-	10.7	-	-	10.7
A907	09:58:21.1	-11:03:22	-	-	-	-	4.5	7.4	7.4	7.7	-	27.0
XMMJ0959	09:59:40.8	+02:31:11	-	-	-	-	-	-	-	8.1	-	8.1
COSMOS-MAMBO	10:00:15.6	+02:15:50	-	23.8	-	41.2	-	-	-	-	-	65.0
RXCJ1023.6+0411	10:23:39.6	+04:11:10	-	-	-	-	8.4	-	-	7.1	-	15.4
MS1054.4-0321	10:56:58.0	-03:37:37	-	-	-	-	1.2	8.5	-	4.0	-	13.7
MACSJ1115.8+0129	11:15:52.1	+01:29:53	-	-	-	-	-	-	15.6	1.9	-	17.5
A1300	11:32:00.7	-19:53:34	0.6	-	-	-	-	10.0	6.1	4.0	-	20.7
XMMJ1132	11:32:32.2	-34:43:50	-	-	-	-	-	-	-	8.4	-	8.4
RXCJ1135.6-2019	11:35:36.8	-20:19:42	-	-	-	-	-	-	11.2	5.8	-	17.0
RXCJ1206.2-0848	12:06:12.2	-08:48:22	-	-	-	-	-	-	6.7	8.1	-	14.8
XMMUJ1229	12:29:29.2	+01:51:26	-	-	-	-	-	3.4	-	-	-	3.4
XMMJ1230	12:30:16.9	+13:39:04	-	-	-	-	-	13.1	10.6	-	-	23.7
RDCS1252.9-2927	12:52:54.4	-29:27:17	-	-	16.3	17.0	-	-	-	-	-	33.4
MACSJ1311.0-0311	13:11:00.0	-03:11:00	-	-	-	-	-	10.1	10.0	5.6	-	25.6
A1689	13:11:29.5	-01:20:17	-	-	-	-	-	9.5	4.3	4.1	-	17.9
RXJ1347-1145	13:47:30.6	-11:45:12	1.2	5.8	2.1	-	1.0	-	-	-	-	10.2
MACSJ1359.2-1929	13:59:10.3	-19:29:24	-	-	-	-	-	9.6	-	-	-	9.6
DLS-F5	13:59:20.0	-11:03:00	-	12.4	-	-	-	-	-	-	-	12.4
A1835	14:01:02.0	+02:51:32	-	-	-	-	-	11.4	-	1.0	-	12.5
RXJ1504	15:04:07.7	-02:48:18	-	-	-	-	-	10.4	-	-	-	10.4
A2163	16:15:45.8	-06:08:55	-	12.0	0.7	-	-	-	-	-	-	12.7
A2204	16:32:45.7	+05:34:43	-	-	-	-	16.6	-	3.7	-	-	20.3
MACSJ1931.8-2635	19:31:48.0	-26:35:00	-	-	-	-	-	9.4	-	-	-	9.4
RXCJ2011.3-5725	20:11:23.1	-57:25:39	-	-	-	-	-	12.0	10.5	-	-	22.5
RXCJ2014.8-2430	20:14:49.7	-24:30:30	-	-	10.1	-	-	-	-	-	-	10.1
MACSJ2046.0-3430	20:46:00.5	-34:30:17	-	-	-	-	-	12.9	-	-	-	12.9
RXCJ2151.0-0736	21:51:01.2	-07:36:03	-	-	-	-	-	-	-	8.1	-	8.1
A2390	21:53:34.6	+17:40:11	-	-	-	-	4.9	0.1	-	-	-	5.0
RXCJ2214.9-1359	22:14:59.0	-13:59:41	-	-	-	-	-	-	-	7.6	-	7.6
XMMXCSJ2215.9-1738	22:15:58.5	-17:38:03	-	-	11.8	-	-	-	-	-	-	11.8
XMMUJ2235.3-2557	22:35:20.6	-25:57:42	-	-	-	-	8.0	21.5	7.6	-	-	37.1
RXCJ2243.3-0935	22:43:20.8	-09:35:18	-	-	-	-	-	-	-	7.1	-	7.1
RXCJ2248.7-4431	22:48:54.3	-44:31:07	-	6.8	-	-	-	-	-	-	-	6.8
AS1077	22:58:52.3	-34:46:55	-	-	-	-	-	16.6	-	-	-	16.6
A2537	23:08:23.2	-02:11:31	-	-	-	-	14.6	0.9	-	-	-	15.5
RCSJ2319.9+0038	23:19:53.2	+00:38:12	-	-	-	-	-	-	9.8	-	-	9.8
BCS2-XMM	23:30:00.0	-55:11:24	-	24.8	-	-	-	-	-	-	-	24.8
RXCJ2337.6+0016	23:37:39.7	+00:17:37	-	-	-	-	-	-	-	9.3	-	9.3
TOTAL HOURS			3.2	88.1	97.6	89.5	45.2	55.2	161.3	181.3	199.0	920.4

- **48 clusters** over a wide range of redshifts
($0.15 < z < 1.5$)
and temperatures
($5 \text{ keV} < kT_e < 15 \text{ keV}$).

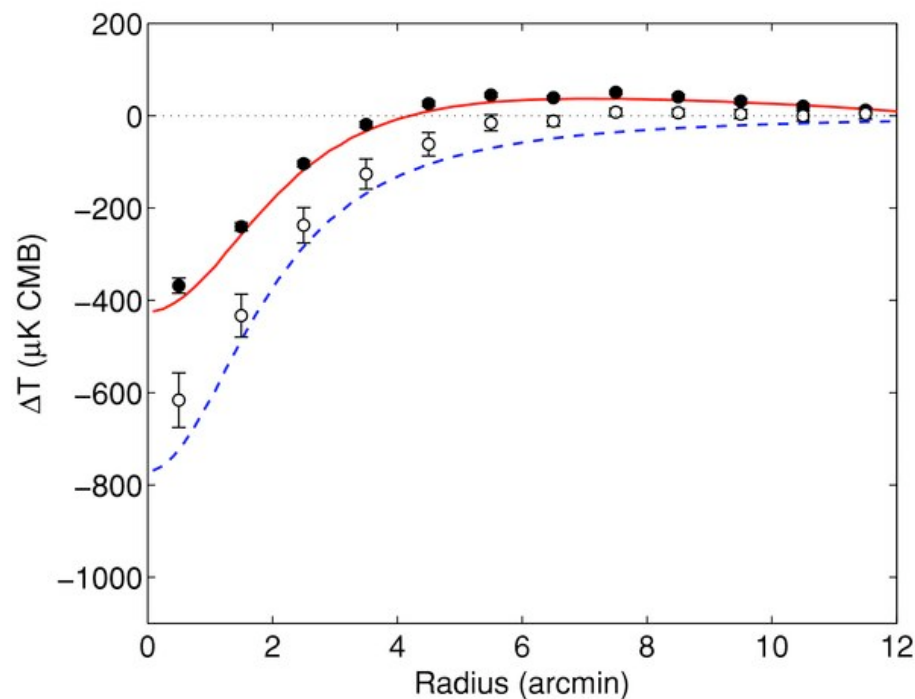
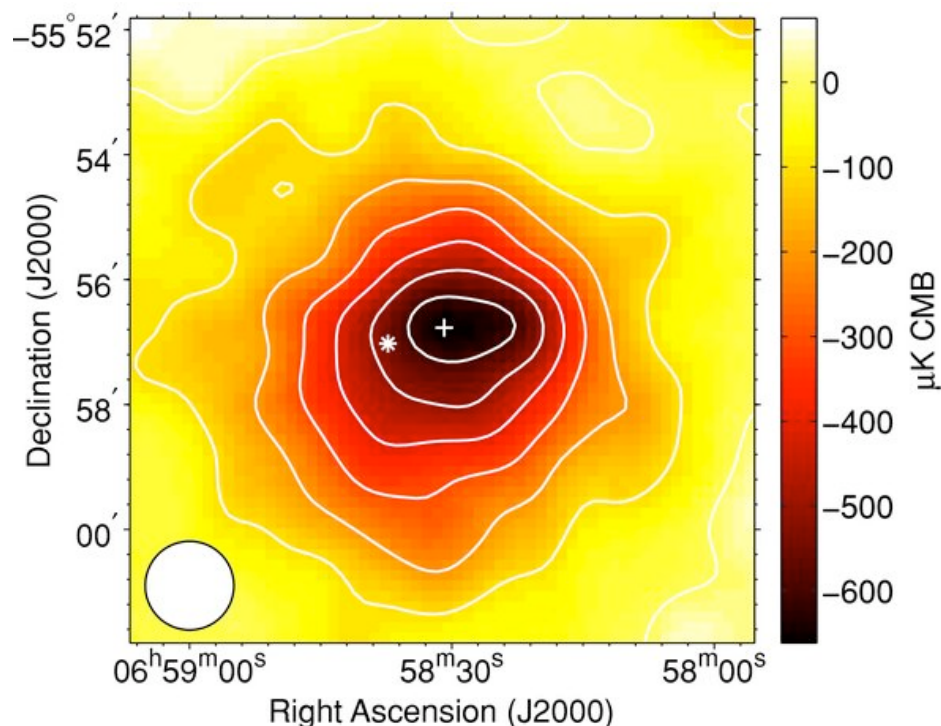
Selected to have X-ray data: 36 XMM-Newton;
8 of the remainder Chandra; 4 REFLEX DXL
($0.26 < z < 0.31$, $L_X > 1.e+45 \text{ erg/s}$ for the 0.1-2.4 keV band

Zhang et al. 2006)

- **2 deep fields** (XMM-LSS and COSMOS)



The Bullet Cluster at $z=0.3$, Halverson et al. 2009



Star: Bright submm galaxy (50 mJy at 870 micron) at $z=2.7$ near a critical line of the Bullet Cluster and magnified 100 times (Johansson et al. 2010); its flux at 2 mm is negligible compared to the SZ

Data points: from 2 different analyses
Blue: best fit

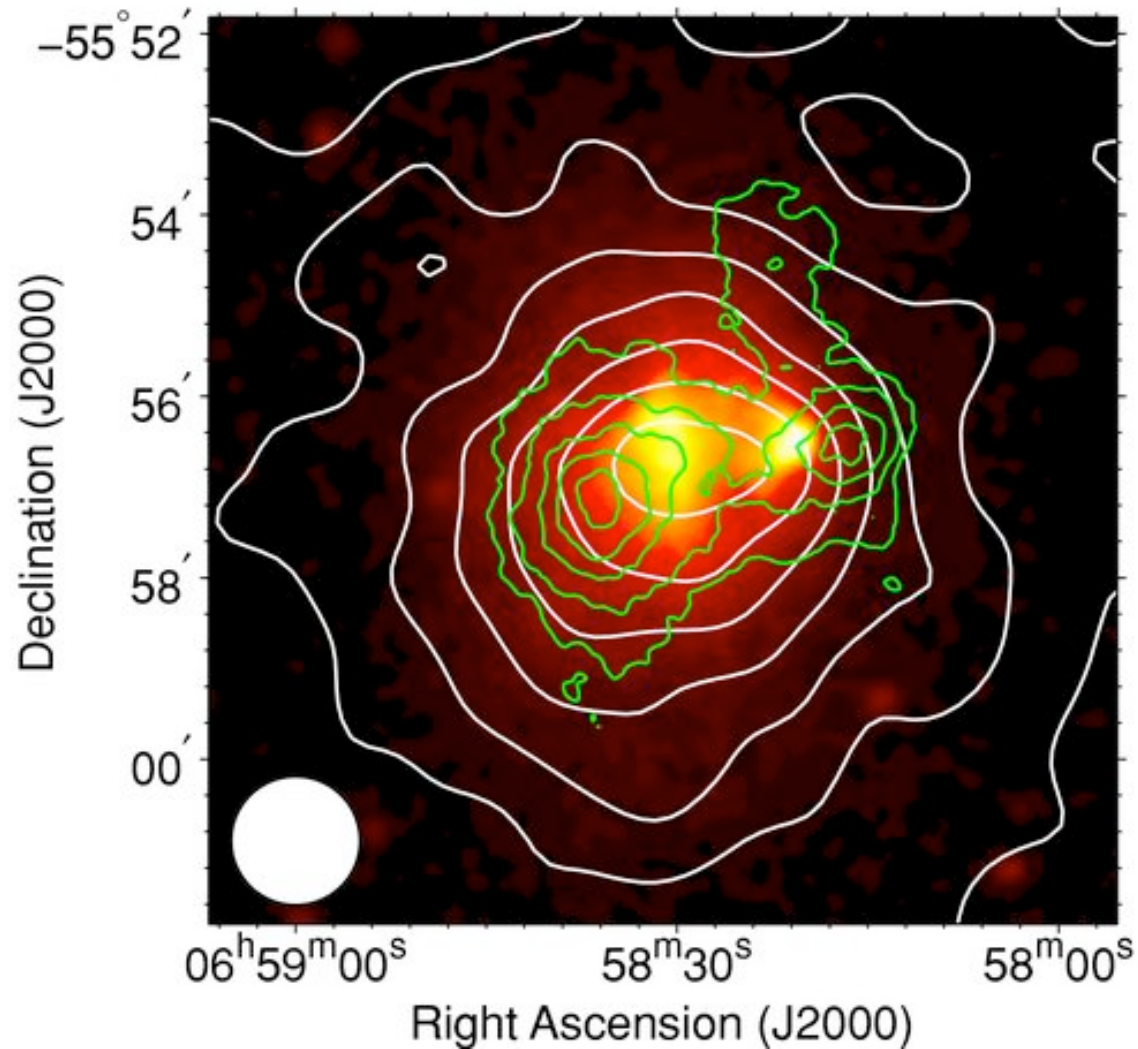
Elliptical beta-model

X-ray-derived prior on $\beta=1.04^{+0.16}_{-0.1}$,

Central SZ decrement: $-771 \pm 71 \mu\text{K CMB}$; $r_c = 142'' \pm 18''$; axial ratio $= 0.889 \pm 0.072$,

Using n_e from Chandra, $T_{\text{mass weighted}} = 10.8 \pm 0.9 \text{ keV}$

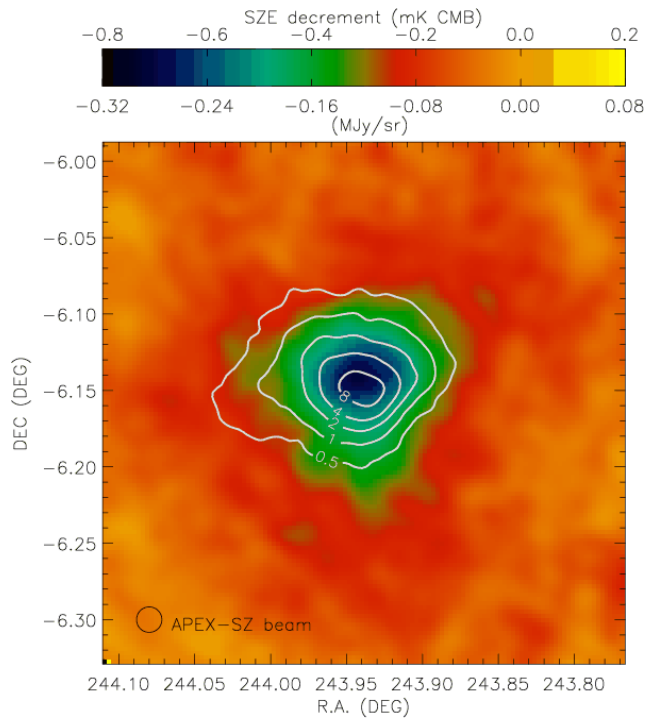
The Bullet Cluster at $z=0.3$, Halverson et al. 2009



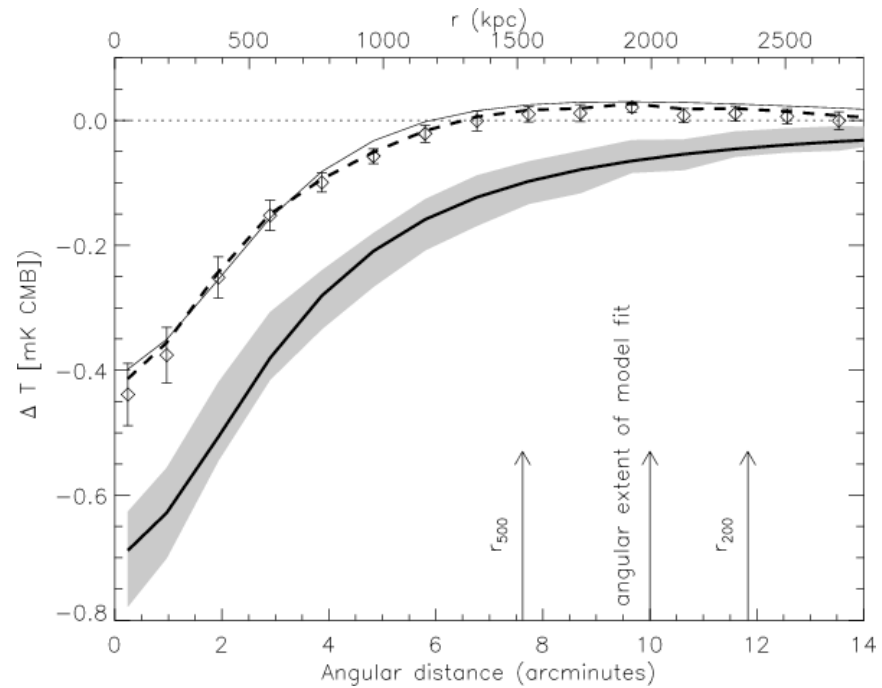
X-ray (color)
+ APEX-SZ (white contours)
+ Weak Lensing (green contours, Clowe et al.)

See Haukur Sigurdarson's talk on Wed
about APEX observations of the SZ increment at 870 micron

Another merging cluster at $z=0.3$, Abell 2163 Nord et al. 2009

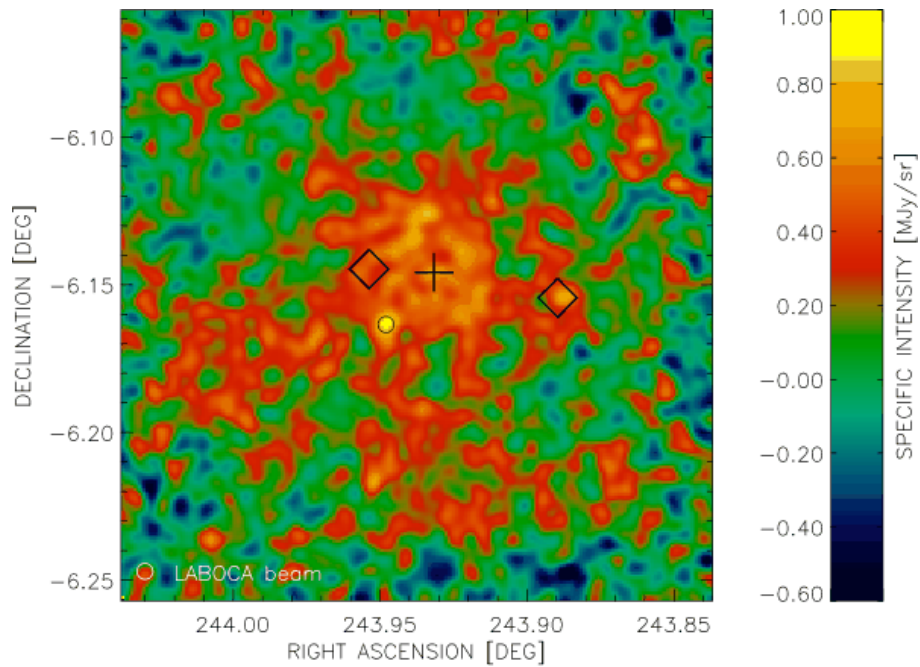


APEXSZ + X-ray (white contours)

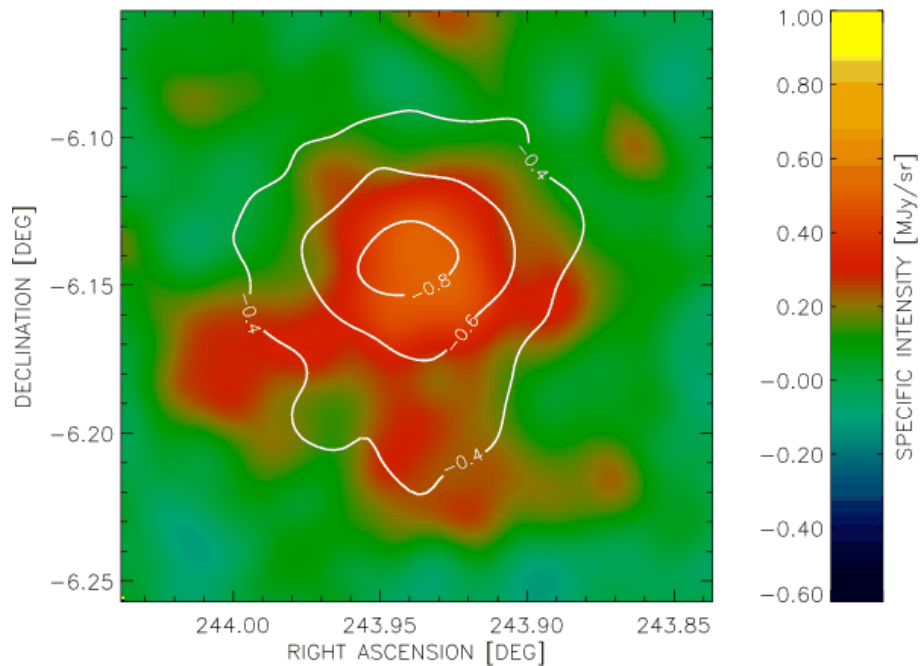


Profile of SZ temperature decrement

Abell 2163 at $z=0.3$, Nord et al. 2009



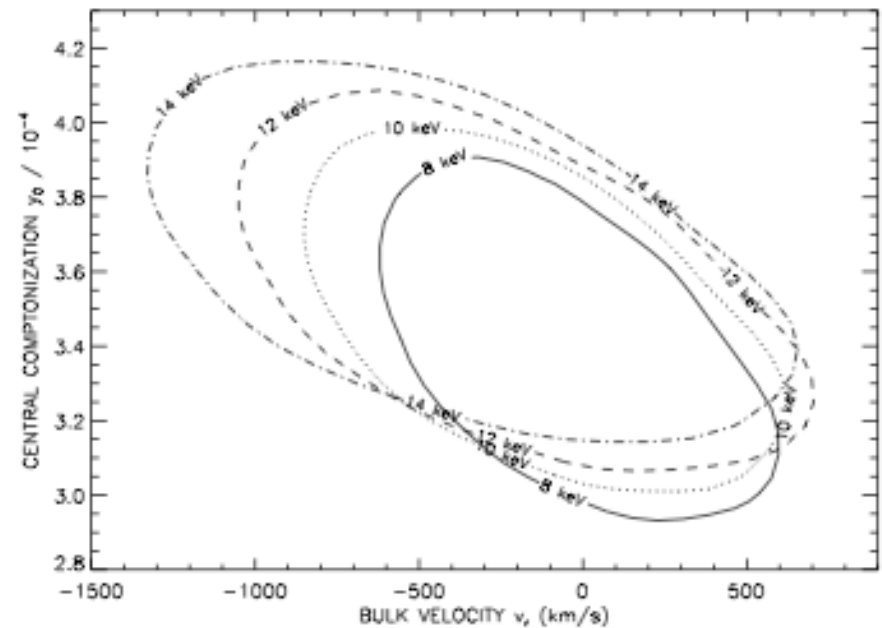
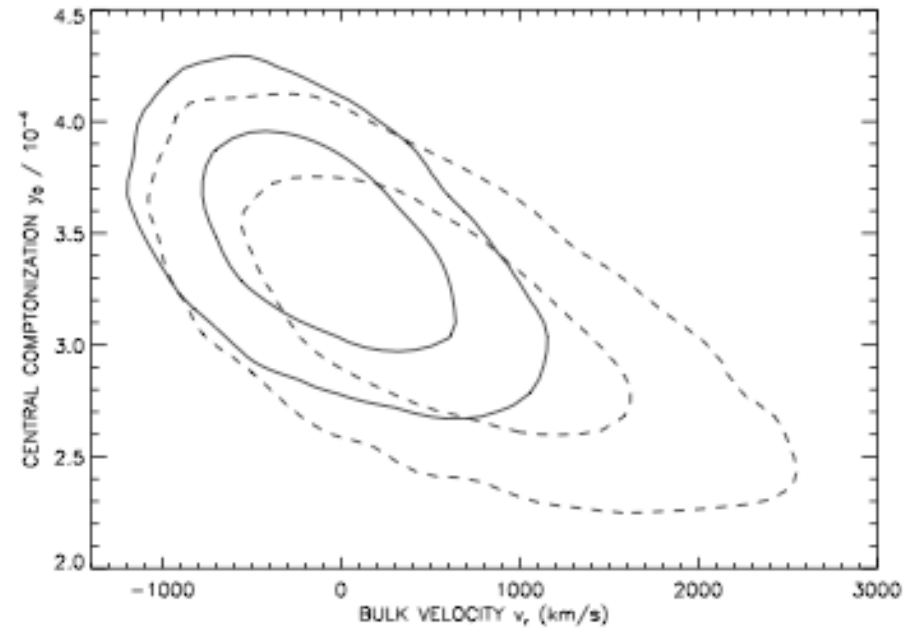
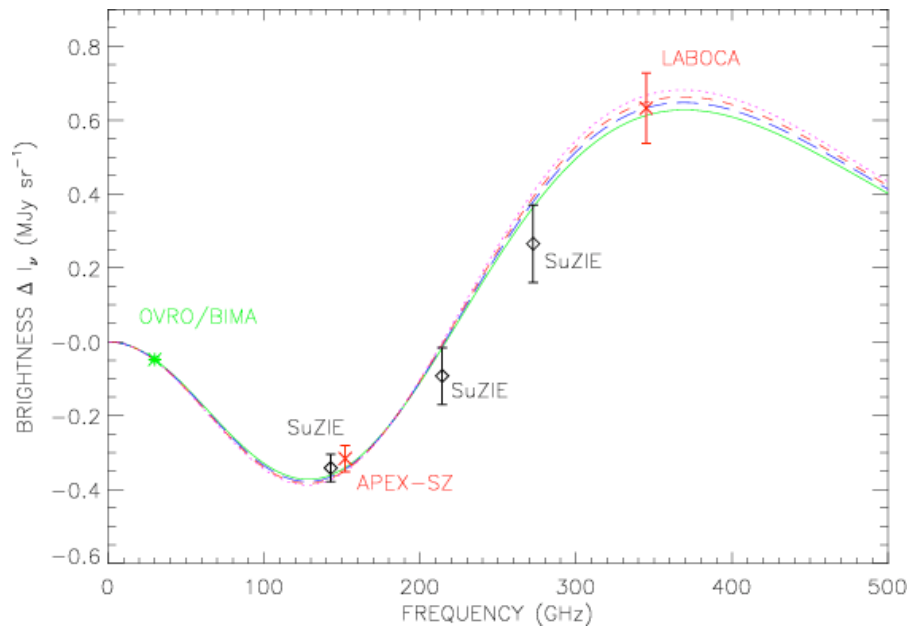
The SZ increment at 350 GHz
+ submm point sources



The SZ increment (color)
+ the **APEX-SZ decrement** (contours)

Abell 2163 at $z=0.3$, Nord et al. 2009

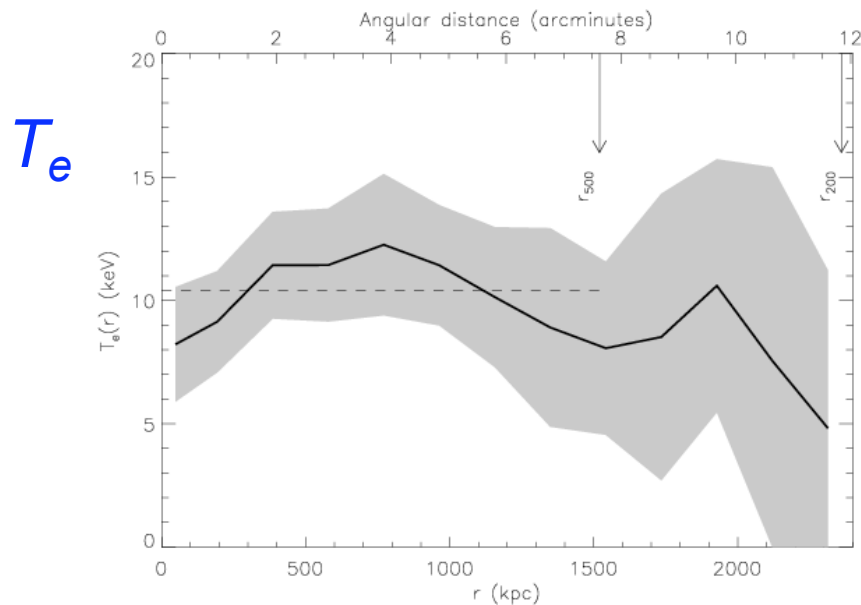
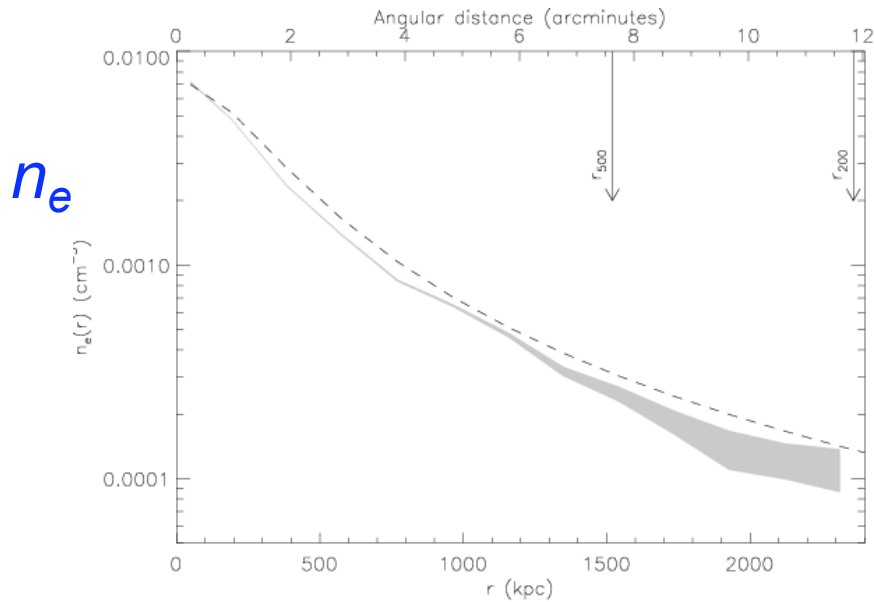
The SZE spectrum



Fixing temperature gives constraint on peculiar velocity-central Compton parameter

Abell 2163 at z=0.3, Nord et al. 2009

De-projected density & temperature



Joint X-ray/SZ analysis:

$$\text{SZ: } \int_{\text{LOS}} n_e T_e dl$$

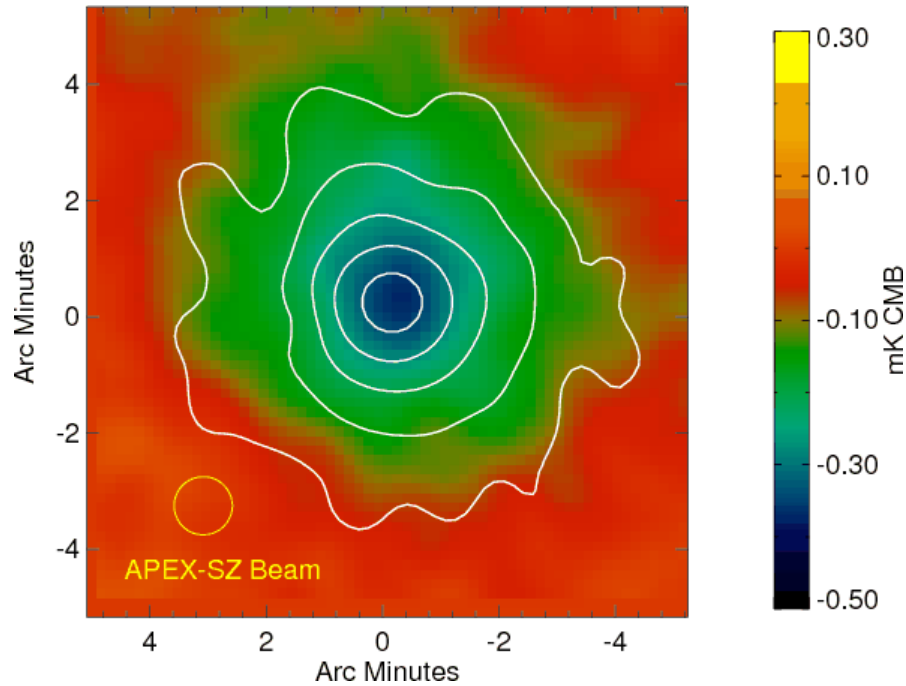
$$\text{X-ray: } \int_{\text{LOS}} n_e^2 \Lambda(T_e) dl$$

Assuming spherical symmetry,
one can use the Abel transformation

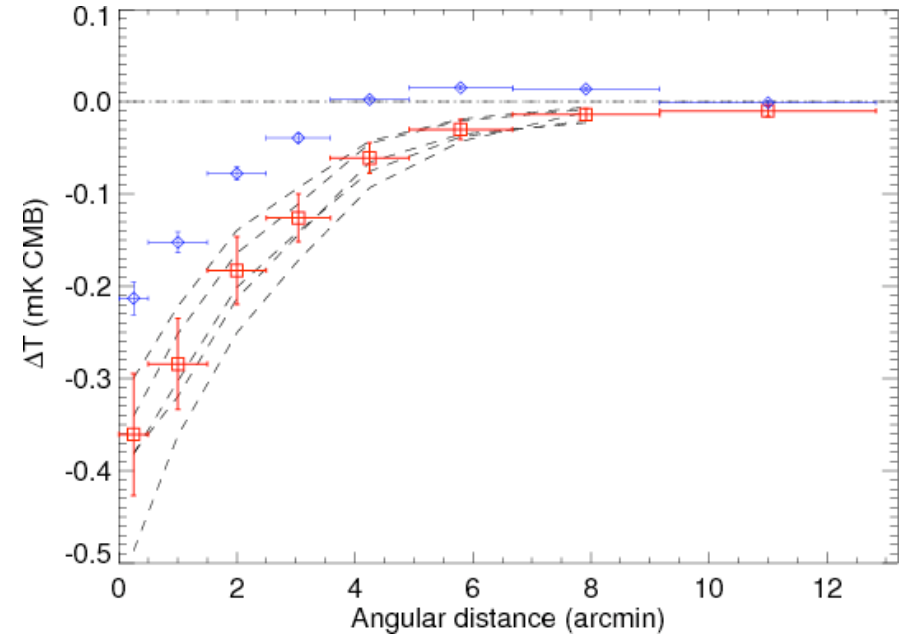
$$T_e(r) n_e(r) = \frac{1}{\pi A_{\text{SZE}}} \int_{\infty}^r \frac{d\Delta T(R)}{dR} \frac{dR}{\sqrt{R^2 - r^2}};$$

$$\Lambda_{\text{H}}(T_e(r)) n_e^2(r) = 4(1+z)^4 \int_{\infty}^r \frac{dS_{\text{X}}(R)}{dR} \frac{dR}{\sqrt{R^2 - r^2}}.$$

A relaxed cluster at $z=0.15$: Abell 2204, Basu et al. 2010



APEX-SZ + X-ray (white contours)



Profile of SZ temperature decrement

Blue: raw profile;

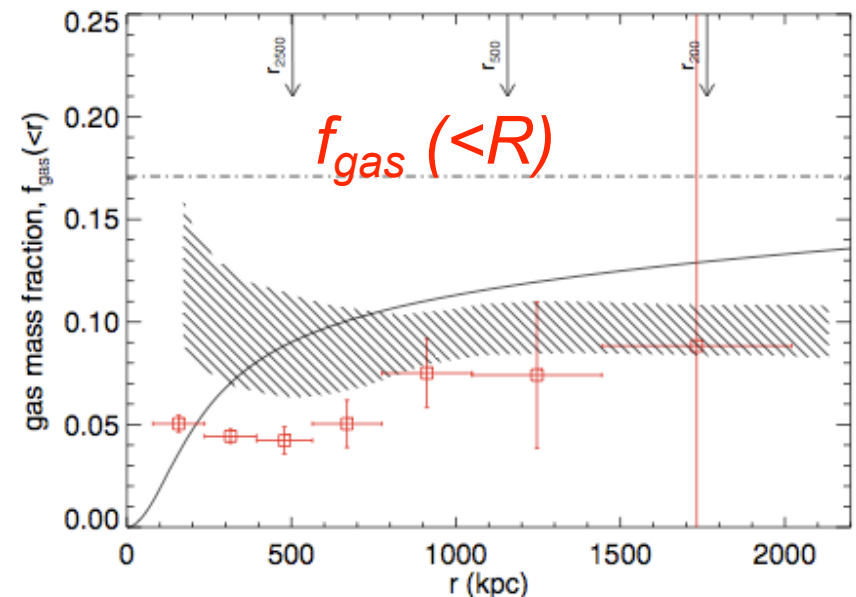
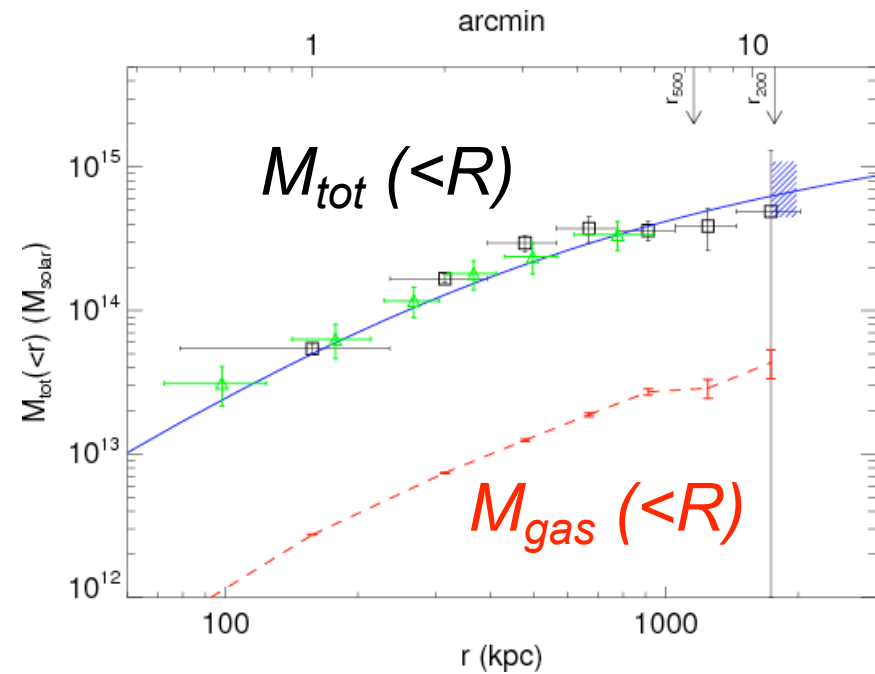
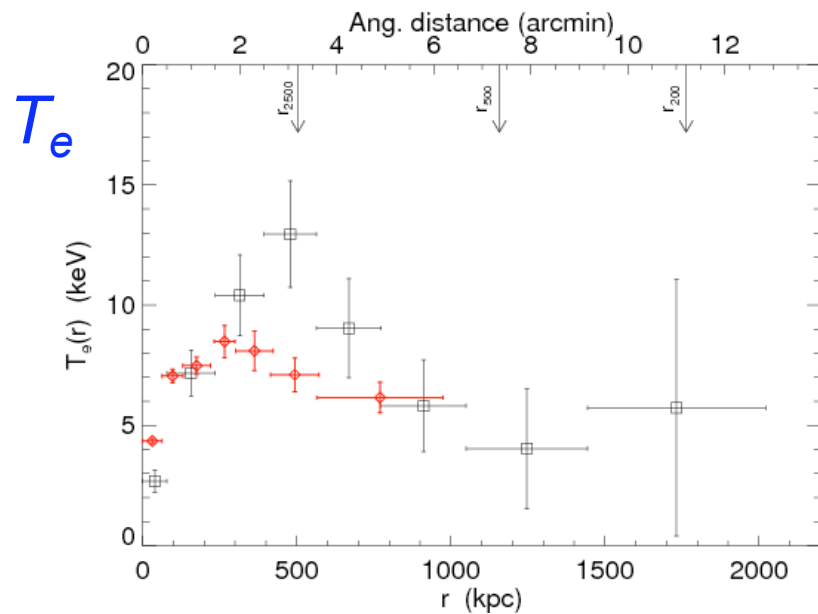
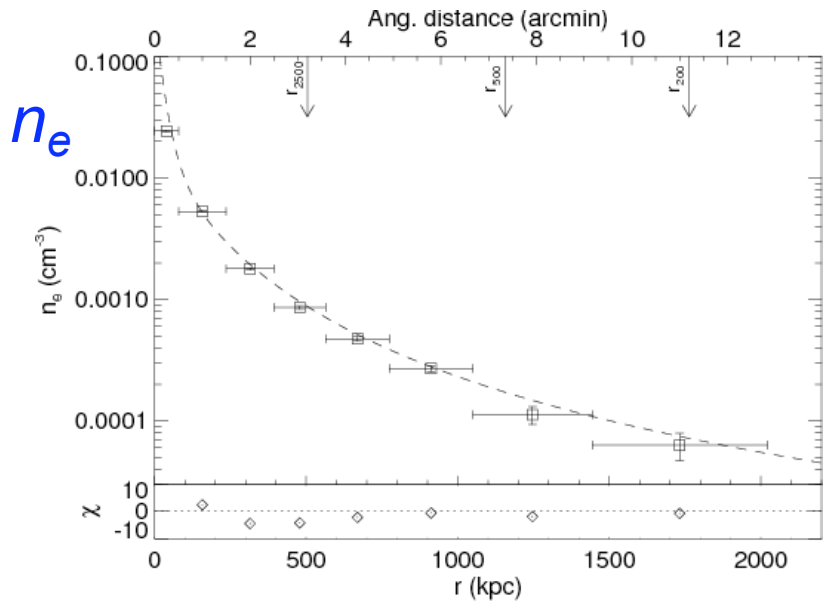
Red: deconvolved from the transfer function

Dashed lines: 5 randomly selected deconvolved profiles

Abell 2204 at $z=0.15$, Basu et al. 2010

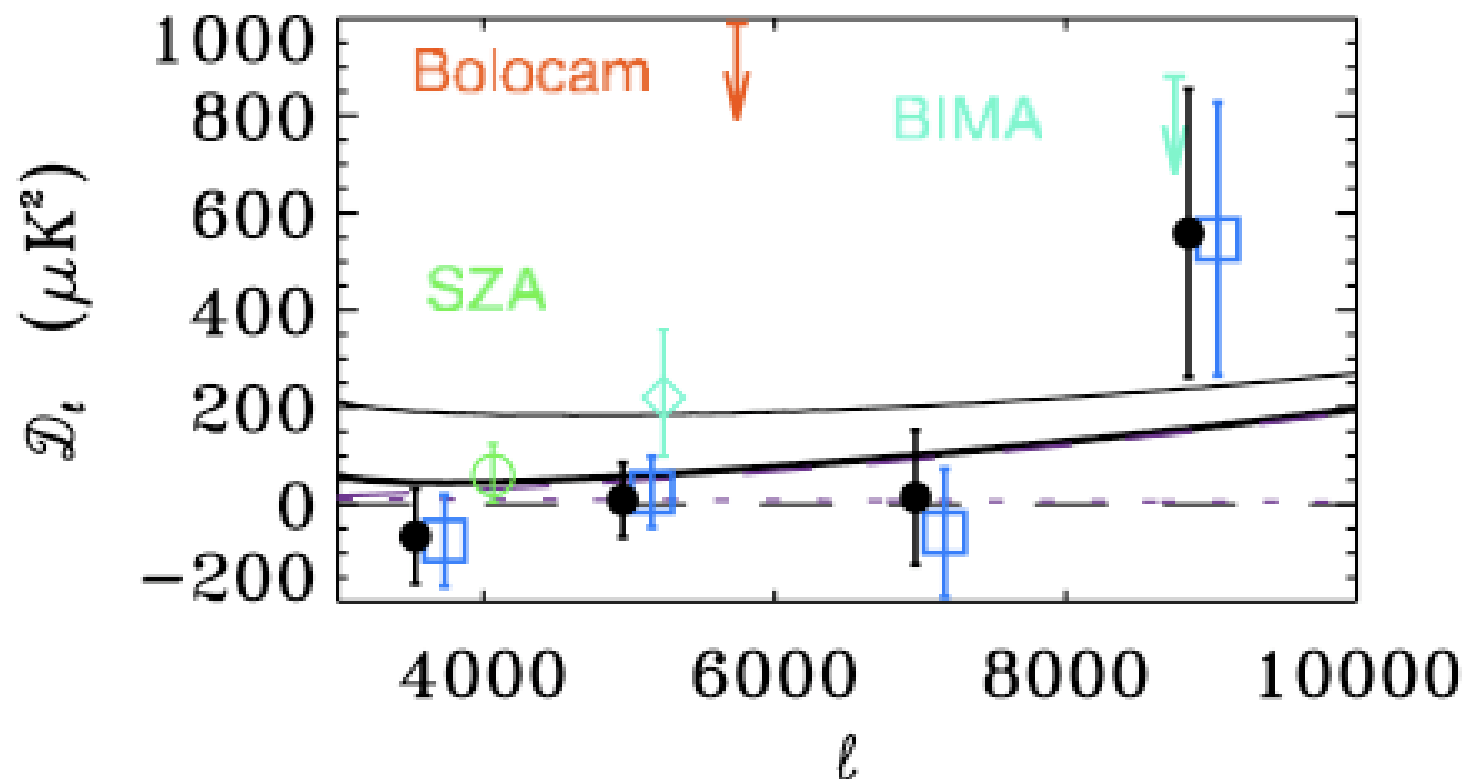
Profile of the enclosed gas mass and the total mass
(assuming hydrostatic equilibrium)

De-projected density & temperature



The APEX-SZ power spectrum at 150 GHz, Reichardt et al. 2009

Derived from a 0.8 square degree map of the central part of the XMM-LSS field, with rms ~ 12 microK



- $3000 < l < 10000$: $1' < \text{angular scale} < 3.6'$
- The power is dominated by dusty submm galaxies
- $\text{sigma}_8 < 1.15$ at 95% confidence

Work in progress

Abell 2744 (“Pandora’s cluster” (!))

$z=0.3$

Collision of 4 subclusters?
(Merten et al. 2011)

Offsets between the gas and
the collisionless dark matter

Red: X-ray

Blue: Mass (lensing)

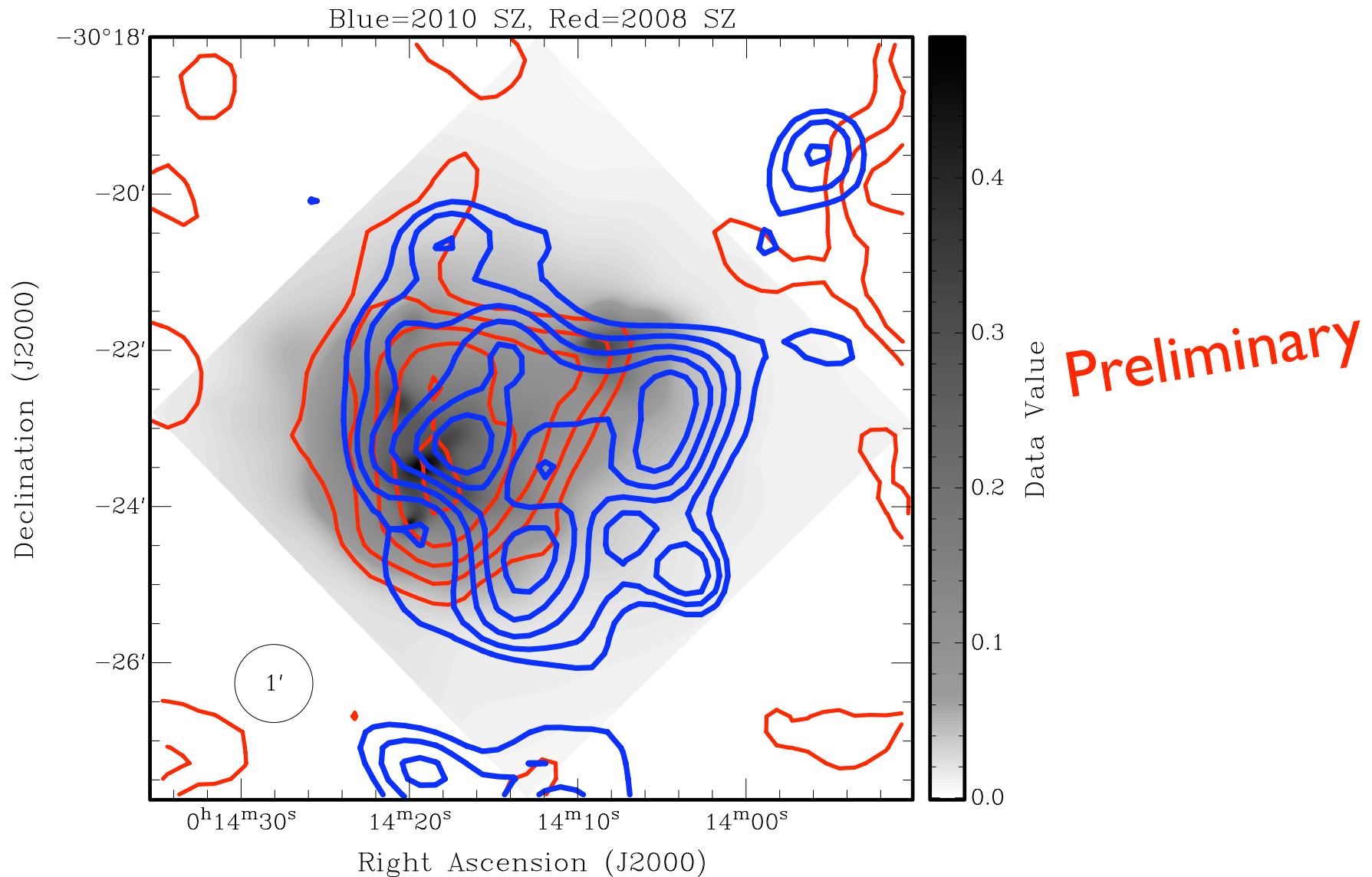
+ Galaxies

(Credit: X-ray: NASA/CXC/
ITA/INAF/J.Merten et al,
Lensing: NASA/STScI; NAOJ/
Subaru; ESO/VLT, Optical:
NASA/STScI/R.Dupke)

2 arcmin

APEX-SZ observations of **Abell 2744** from 2008 and 2010

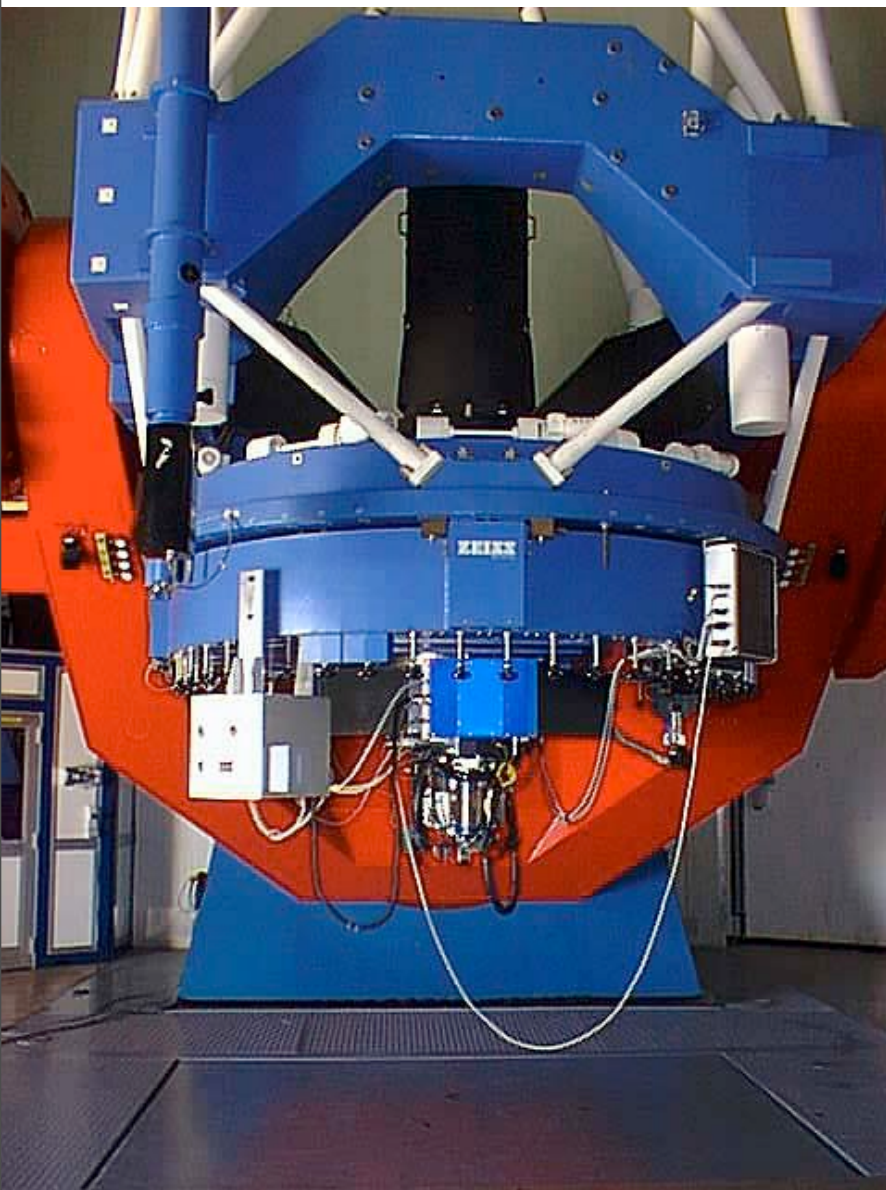
Different scanning patterns (and transfer functions) to recover more extended emission



Background: X-ray from Chandra

Lensing follow-up (PhD of Matthias Klein, Bonn)

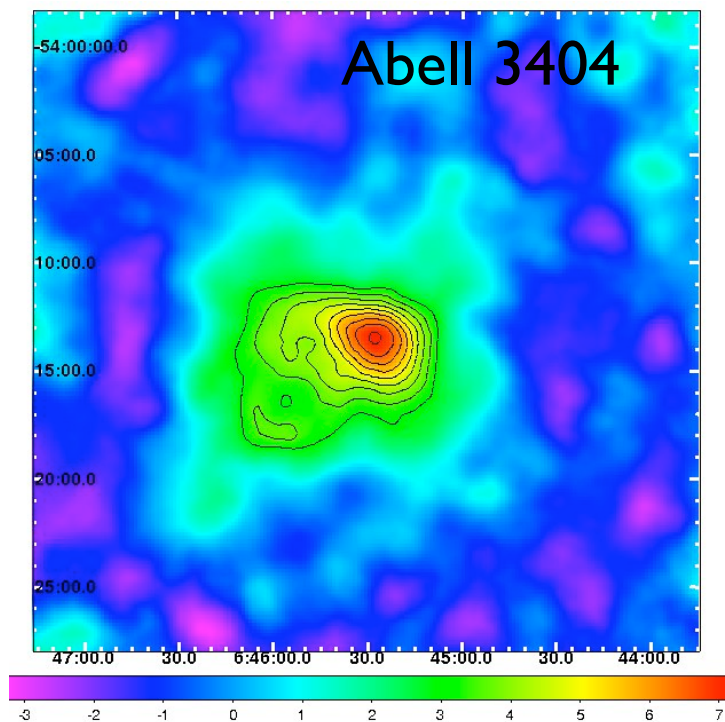
BVR observations with the wide field imager (WFI) on the ESO/MPG 2.2 m telescope in La Silla, FOV = 33'x34'



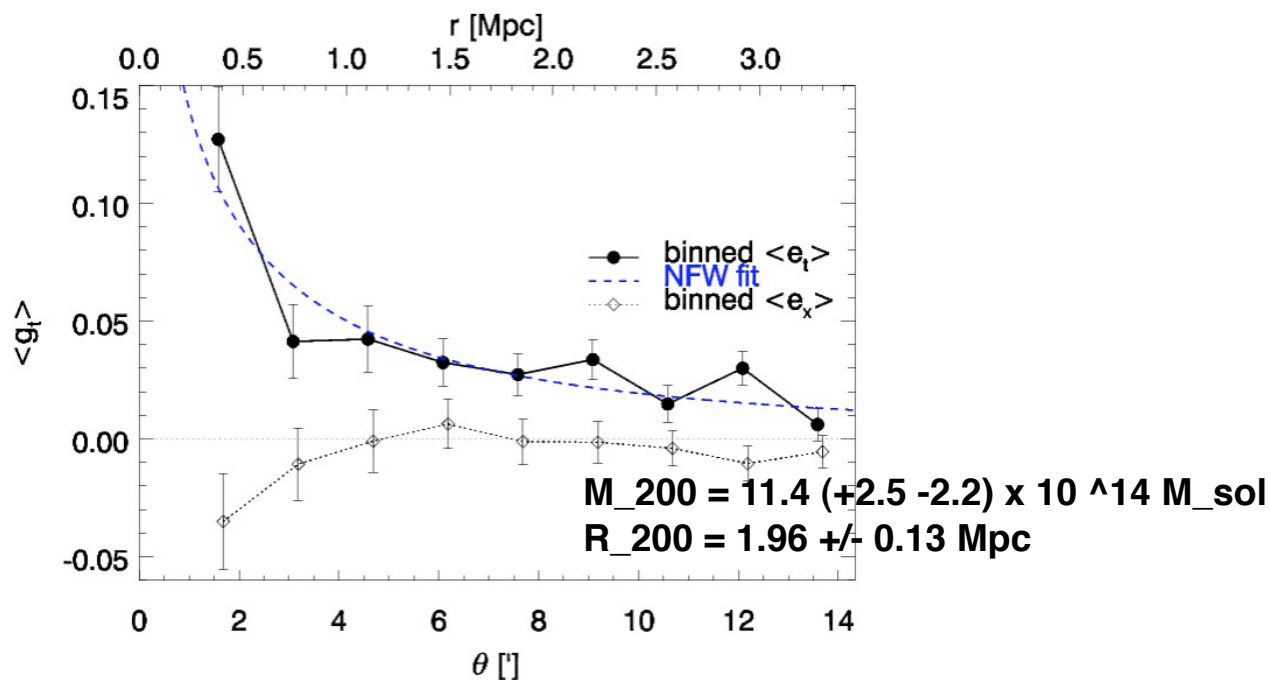
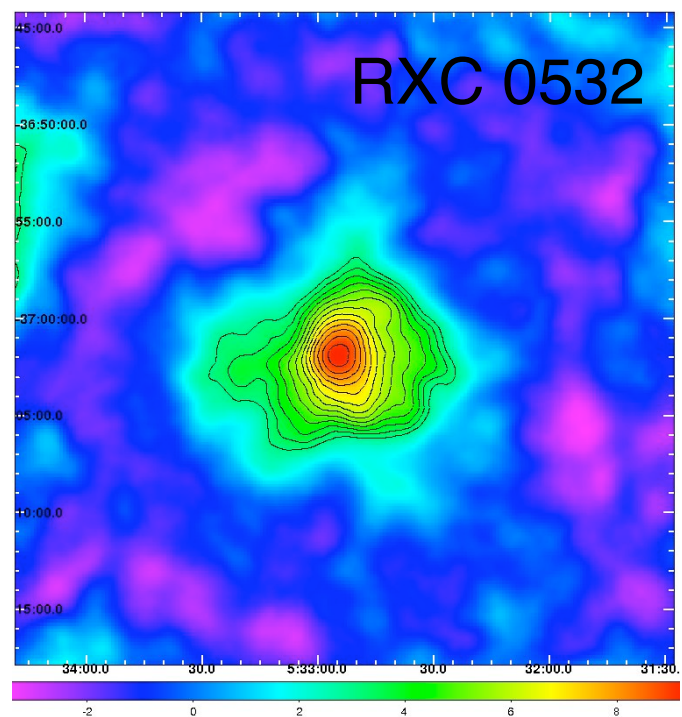
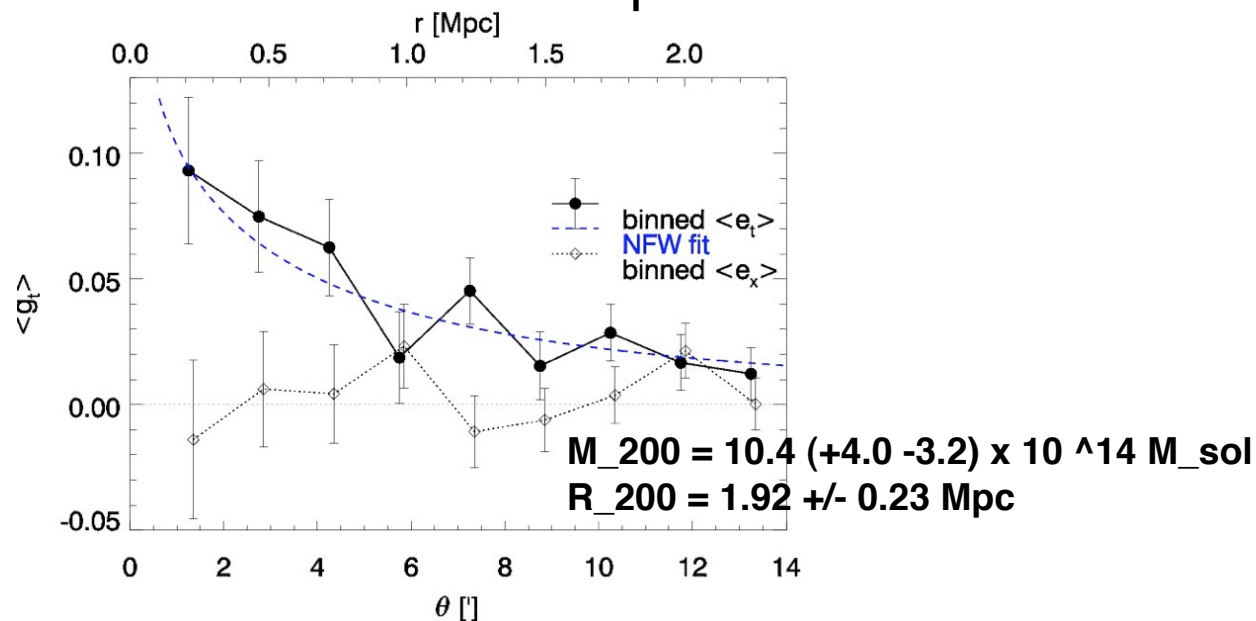
Weak lensing follow-up of the **15 clusters** of our sample for which no WL data exist in archives.

7 clusters were observed so far.

Ongoing PhD work of Matthias Klein (Bonn)



S/N maps of the reconstructed projected mass and shear profiles



Scaling relations (PhD of Amy Bender, Colorado)

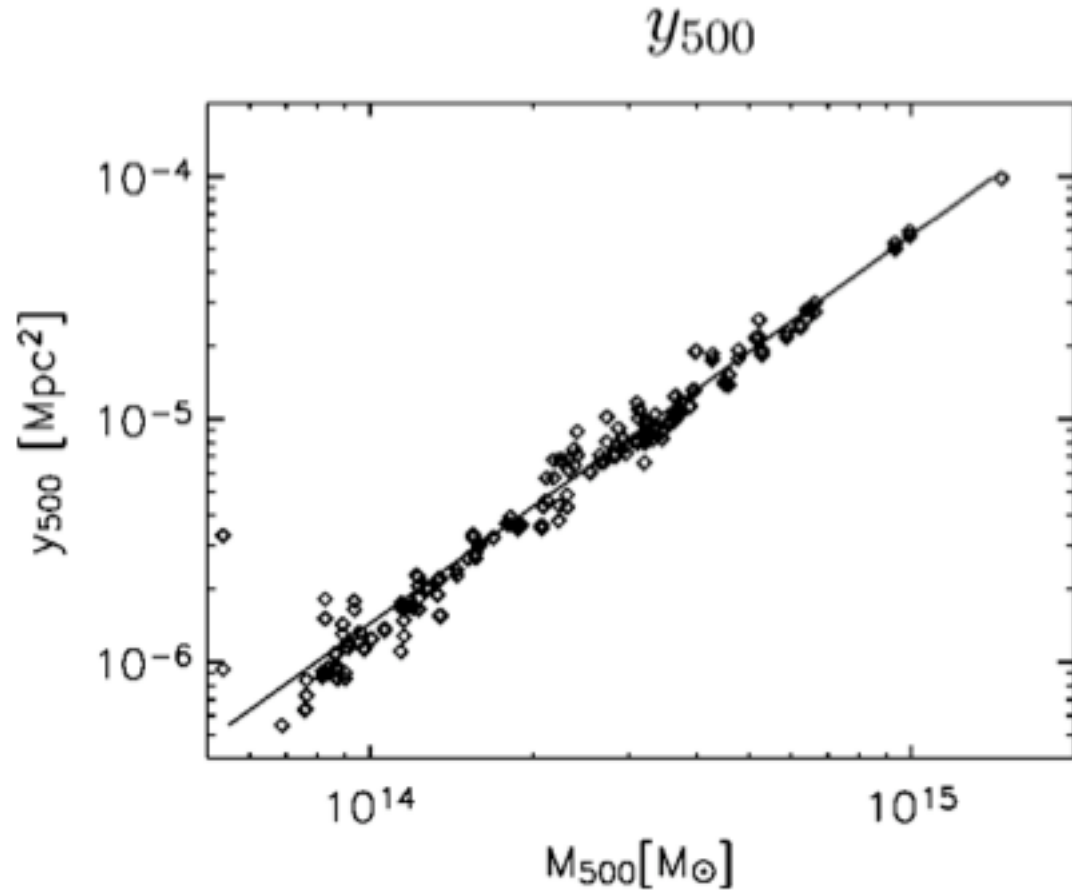
The integrated Compton parameter Y_{sz} is a good proxy of the cluster's total mass;
e.g. Arnaud et al. 2010; Motl et al. 2006:

Self-similarity:

$$Y \sim T^{5/2}$$

$$Y \sim M^{5/3}$$

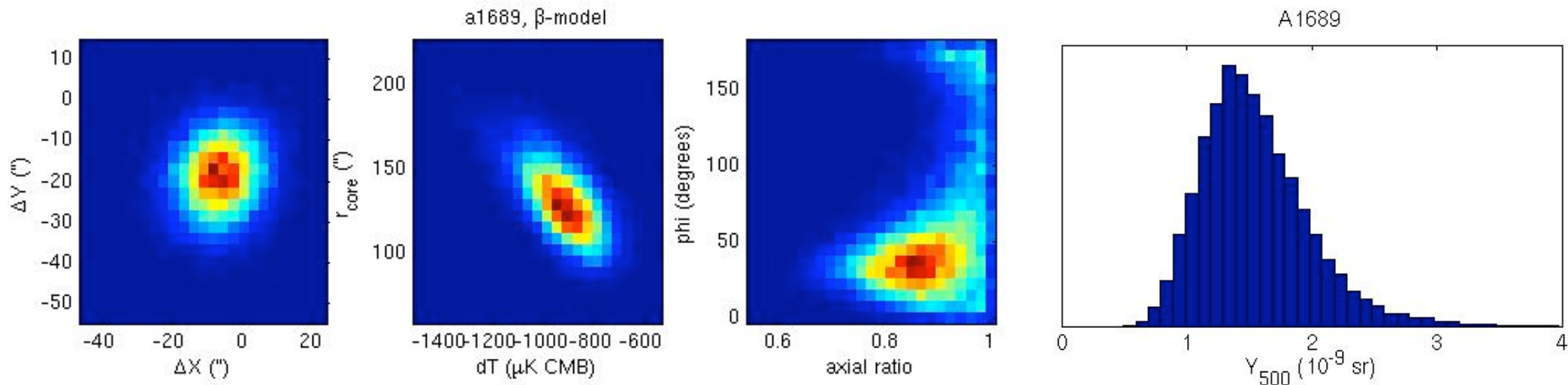
$$Y \sim M_{\text{gas}}^{5/3}$$



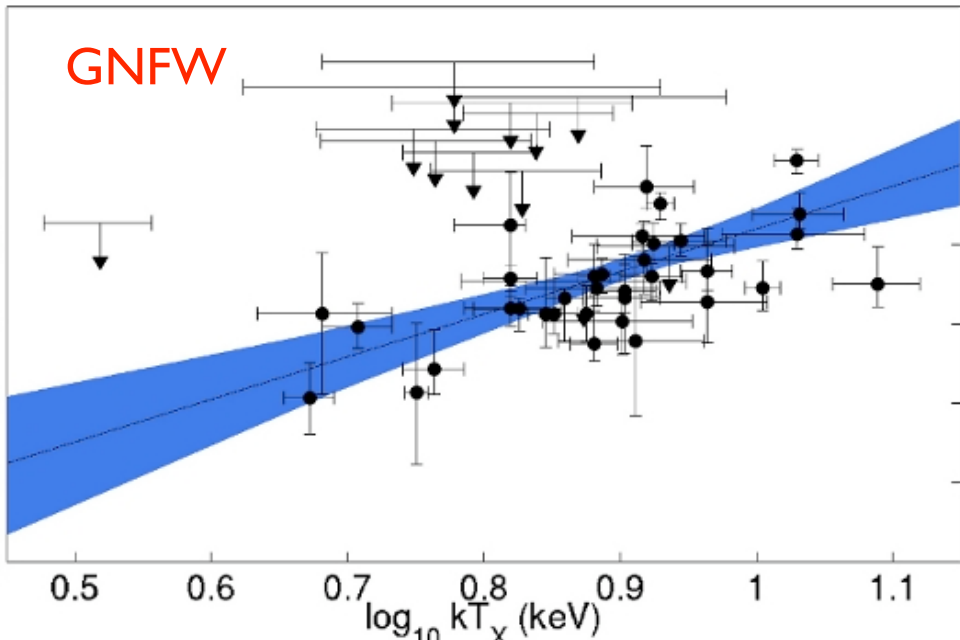
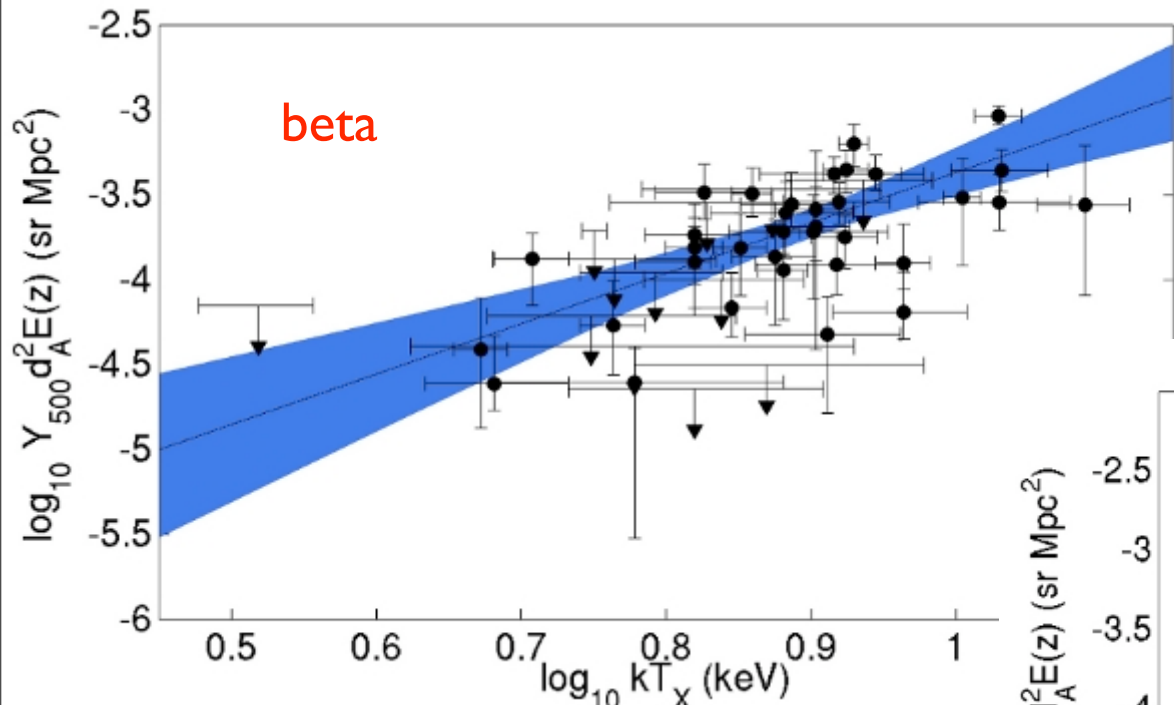
APEX-SZ scaling relations - Measuring Y_{500}

From Amy Bender's work

- 2 models of the intracluster gas:
 - Isothermal beta-model
 - Generalized NFW
- The likelihood of Y_{500} is estimated from parameter fitting, using jackknife maps (half the dataset minus other half, randomly) to model the noise



From Amy Bender's work



Preliminary

Table 4.3. Linear Regression Parameters

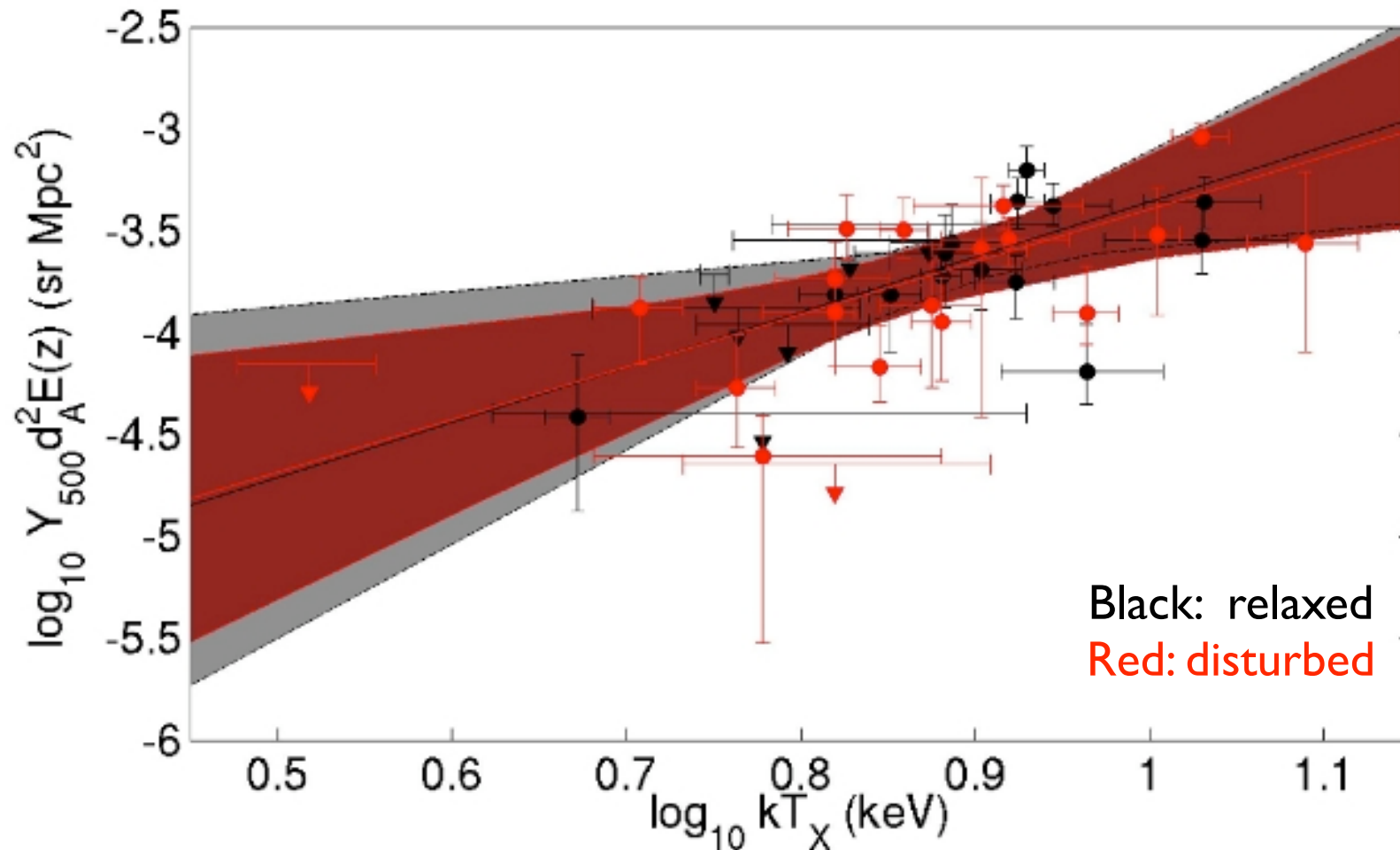
Subset	Isothermal β -model			GNFW Model		
	A	B	$\sigma_{Y,int}$	A	B	$\sigma_{Y,int}$
All Clusters	$-6.31^{+0.60}_{-0.58}$	$3.08^{+0.56}_{-0.78}$	$0.19^{+0.07}_{-0.04}$	$-6.11^{+0.55}_{-0.49}$	$2.72^{+0.54}_{-0.61}$	$0.18^{+0.04}_{-0.05}$
Relaxed Only	$-6.00^{+1.11}_{-1.24}$	$2.50^{+1.50}_{-1.11}$	$0.19^{+0.08}_{-0.09}$	$-6.34^{+0.68}_{-1.06}$	$3.10^{+1.07}_{-0.88}$	$0.12^{+0.08}_{-0.04}$
Disturbed Only	$-5.88^{+0.75}_{-1.04}$	$2.77^{+0.88}_{-1.15}$	$0.27^{+0.08}_{-0.10}$	$-5.79^{+0.91}_{-0.71}$	$2.36^{+0.78}_{-1.09}$	$0.25^{+0.09}_{-0.07}$
Disturbed+Unknown	$-6.09^{+0.66}_{-0.95}$	$2.84^{+0.89}_{-0.96}$	$0.27^{+0.08}_{-0.09}$	$-5.84^{+0.87}_{-0.72}$	$2.25^{+0.93}_{-0.83}$	$0.22^{+0.10}_{-0.05}$
REFLEX-DXL	$-5.68^{+1.22}_{-0.98}$	$2.19^{+1.15}_{-1.37}$	$0.26^{+0.11}_{-0.08}$	$-5.93^{+0.88}_{-0.77}$	$2.56^{+0.82}_{-1.08}$	$0.19^{+0.09}_{-0.06}$
Point Source Cut	$-6.29^{+0.64}_{-0.56}$	$2.96^{+0.60}_{-0.74}$	$0.21^{+0.05}_{-0.08}$	$-5.94^{+0.44}_{-0.61}$	$2.57^{+0.62}_{-0.53}$	$0.16^{+0.05}_{-0.05}$

Effect of dynamical state

Simulations indicate that Y is rather insensitive to dynamical state (e.g. Kravtsov et al. 2006, Poole et al. 2007)

APEX-SZ scaling relations

From Amy Bender's work



Contaminating point sources? *(Ben Westbrook's PhD work)*

Some of our upper limits on the SZ signal are not consistent with predictions from X-ray measurements.

=> Could a point source 'fill' the SZ decrement?

CARMA program to observe the 3mm and the 1mm of clusters

- marginally detected or undetected by APEX-SZ
- with a bright NVSS source near the cluster's X-ray position

In particular, we detected only 1 out of 4 high- z clusters:

* XMMU J2235.3-2557, $z = 1.393$ (Mullis et al. 2005; SZ from Culverhouse et al. 2010, SZA)

XMMXCS J2215, $z = 1.45$ (Hilton et al. 2007)

RDCS1252.9-2927, $z = 1.23$ (Rosati et al. 2003)

XMMU J1230.3+1339, $z = 0.975$ (Fassbender et al. 2011)

Future work

SZ: ALMA/ ACA, CCAT

**LOFAR observations of the radio continuum in galaxy clusters
(radio halos and relics)**

LOFAR: Low Frequency Array, $\lambda > 1.5$ m (15-80 MHz, 120-200 MHz)
Mostly Dutch (36 stations), and international participation
(5 stations in Germany, 1 in UK, 1 in France, 1 in Sweden)

A survey instrument: FOV: 1-10 deg.

Goal: Survey the whole Northern sky ($\text{DEC} > 0$) at 15, 30, 60 and 120 MHz, and selected areas at 200 MHz.

Later: Even the XXL $\text{DEC} = -5$ deg field.

- Galaxy clusters (radio halos and relics)
- Distance radio galaxies (ca 100 at $z > 6$) AGN, starburst galaxies



Onsala LOFAR station completed
Will be inaugurated on Sep 26, 2011



GMRT 150 MHz observation of giant double radio relic in Planck SZ-detected cluster PLCKG287.0+32.9 at $z=0.39$
(Bagchi et al. 2011 April 29, arxiv)

